Reaction Chemistry & Engineering

ROYAL SOCIETY OF CHEMISTRY

PAPER

View Article Online
View Journal | View Issue

Cite this: *React. Chem. Eng.*, 2024, 9, 1173

Elucidation of the kinetic stabilities of carbenoid species by integration of theoretical and experimental studies†

Kazuhiro Okamoto, [a] Kensuke Muta,[b] Hidetaka Yamada, [c] Ryosuke Higuma,[d] Yosuke Ashikari [a] and Aiichiro Nagaki *[a]

Received 1st December 2023,
Accepted 10th January 2024

DOI: 10.1039/d3re00648d

rsc.li/reaction-engineering

The flash quench-flow kinetics of short-lived intermediates such as lithium halocarbenoids have revealed precise kinetics even in subsecond-order reactions. Simple quantum calculations dealing with the bond dissociation energies of the carbon–halogen bond in lithium carbenoid intermediates and their statistical comparison with experimental kinetic data exhibited strong correlations, predicting the decomposition rates for various dihalomethanes.

Carbenoid species are highly valuable for organic synthesis because they can be used in sequential reactions owing to their ambivalent and bifunctional reactivity. The generation of C1 carbenoid species from dihalomethanes with strong bases is recognized as a universal method for C1 unit elongation because it does not require the assistance of transition metal catalysts with complex structures (eqn (1)).[1] Such methods for carbenoid generation display remarkably high performance in sequential homologation reactions, such as Matteson's method (eqn (2)).[2] Considering the extreme instability of the lithium carbenoid intermediates, the usual protocols for boronate homologation reactions are conducted in the presence of a subsequent organoboron reagent under cryogenic conditions. Despite the synthetic utility of the carbenoid species, the aforementioned experimental regulations for their manipulation using conventional experimental approaches have made the elucidation of the reactivity parameters difficult.

Recently, quantum calculations have been widely studied for estimating the reactivity of active species that are unstable in their isolated form. Transition-state energy calculations are typically employed to evaluate reactivities by obtaining the energy diagram of each reaction pathway.[3] Generally, the exploration of transition states and estimation of activation energies reveal the kinetic reactivities of the active intermediates in each pathway by using energy diagrams. Many methods have been developed to date, and recent studies have focused on more comprehensive and objective exploration methodologies, such as the AFIR (artificial force induced reaction) method, to elucidate the overall reactivities of active species that are difficult to predict.[4] However, with such methodologies, various difficulties remain in estimating the stability of highly active species, such as metal carbenoids.

$$\underset{\mathbf{1}}{CH_2X^1X^2} + LiNiPr_2 \rightarrow \underset{\mathbf{2}}{LiCHX^1X^2} + HNiPr_2 \quad (1)$$

$$\underset{\mathbf{2}}{LiCHX^1X^2} + \underset{\mathbf{3}}{R\text{–}B(OR)_2} \rightarrow \underset{\mathbf{4}}{R\text{–}CHX^1\text{–}B(OR)_2} + Li\text{–}X^2 \quad (2)$$

First, the reactivities of carbenoids are too high to construct comprehensive prediction models because of the many decomposition pathways, including intermolecular dimerisation or oligomerisation reactions, electron transfer, and generation of radical species.[5] Second, even if a nanoscale estimation of their reactivities at the unimolecular level can be performed, the actual reactions of highly polarised carbenoid species are strongly affected by mesoscale interactions such as solvation and molecular assembly.[6] Therefore, the estimation of such species is not always clear in the current regime of prediction models. Third, reliable calculation models for reactive intermediates often incur huge computational costs because they should include not only quantum calculations but also the essence of molecular dynamics. Therefore, this approach hinders the

[a] *Department of Chemistry, Graduate School of Science, Hokkaido University, Sapporo 060-0810, Japan*
[b] *Fundamental Chemical Research Center, Central Glass Co., Ltd., 17-5, Nakadai 2-chome, Kawagoe City, Saitama 350-1159, Japan*
[c] *Frontier Science and Social Co-creation Initiative, Kanazawa University, Kakuma-machi, Kanazawa, Ishikawa 920-1192, Japan*
[d] *Department of Synthetic and Biological Chemistry, Graduate School of Engineering, Kyoto University, Nishikyo-ku, Kyoto 615-8510, Japan*

† Electronic supplementary information (ESI) available: Experimental details, compounds characterisation data, and NMR spectra. See DOI: https://doi.org/10.1039/d3re00648d

construction of realistic calculation models that can be expanded to a more generalized system for the estimation of active species.

While many methods for measuring the kinetic rates of active species have been developed, experimental elucidation of reactivities for unstable intermediates is difficult, not merely because these are the kinetically "fast" reactions. The reactivity and stability of the active species are usually complex, and their actual behaviour is composed of a complex combination of very fast physical and/or chemical processes, including premixing, generation, self-assembly, decomposition, oligomerization, and the target reaction. Conventional approaches utilising experimental kinetic analyses are not sufficient to solve such complexities in organic syntheses dealing with short-lived intermediates, and a more integrated methodology combining calculation chemistry and data science is desired. Hence, our research target is to establish systematic and practical estimation methodologies by merging experimental and theoretical studies with statistical modelling.[7] Once flash and continuous-flow organic chemistry are organically connected to quantum chemistry calculations as well as mathematical data analyses, this methodology will provide a new reaction theory based on the digitalized reaction parameters obtained by time–space separation on the order of subseconds, which further leads to the accurate prediction of intermediate reactivities.[8–10]

In this study, we disclosed the comprehensive reactivities and stabilities of lithium halocarbenoids by merging space–time-separated fast-flow reaction systems and theoretical correlations from *ab initio* quantum calculation models.[11] Notably, this study overcomes the limitations of both experimental and theoretical investigations using statistical evaluations based on simple calculation models.

At the beginning of this research, we hypothesised that a very simple calculation model based on the homolytic dissociation of a C–X bond in lithium carbenoid intermediate **2** ($LiCHX^1$–X^2) correlates to the kinetic decomposition rate of **2** in a very fast experimental system. To obtain high-quality data on the kinetic decomposition rates over a short period of time, we set up a microflow reaction system for deprotonation by LDA under rapid mixing conditions (flow rate = 6.0 mL min^{-1}), followed by internal quenching with methanol-d_4 (Scheme 1). Therefore, we obtained kinetic data for the decomposition of **2** indirectly from the decrease in the yield of the monodeuterated product **7** (eqn (3)). Our investigations into the decomposition behaviour of lithium carbenoids began with the measurement of the decrease in deuteration yields at −20 °C during the time range of 0.069 to 15.7 s.

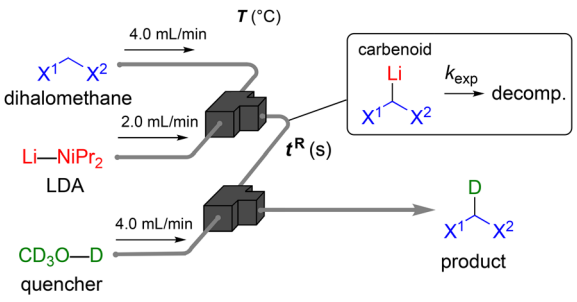

Scheme 1 Reaction sequence of dihalomethane (**2**) based on a flash quench-flow method using a flow microreactor. Standard reaction conditions: dihalomethane (0.10 M in THF), LDA (0.42 M in THF), and methanol-d_4 (0.30 M in THF).

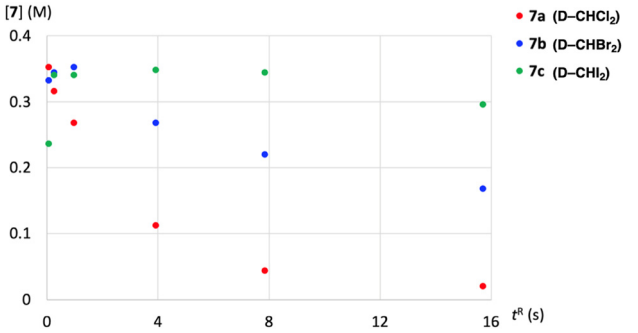

Fig. 1 Time-dependent generation/decomposition behaviours for dihalomethyllithium from dihalomethanes with two identical halogen atoms by plotting the yields of the corresponding deuterated products **7a–c**. Conditions: T = −20 °C. t^R = 0.069, 0.27, 0.98, 3.9, 7.9, 16 s.

$$\underset{\mathbf{2}}{LiCHX^1X^2} + CD_3OD \rightarrow \underset{\mathbf{7}}{CHDX^1X^2} + CD_3OLi \quad (3)$$

The reaction behaviors of dichloro- (**2a**), dibromo- (**2b**), and diiodomethyl- (**2c**) lithium reagents were quantified by illustrating the yields of deuterated products **7a–c** (Fig. 1). While the amount of **7c** exhibited a monotonic decrease with an exponential curve for **7a** and **7b**, an increase in the yield was observed at the early stage of the reaction, and the yields decreased rapidly after reaching a maximum. We assumed that the decrease in yields after the maximum was due to the

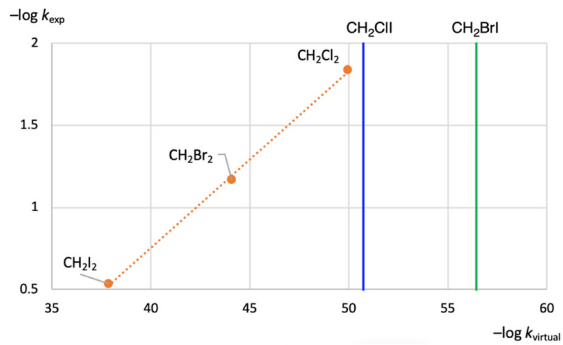

Fig. 2 Linear regression for experimental ($-\log k_{exp}$) and theoretical ($-\log k_{virtual}$) kinetic rates for decomposition of lithium halocarbenoids bearing two identical halogen atoms ($X^1 = X^2$ = Cl, Br, I). Estimation of the trend for the dihalomethyllithium species containing at lease one iodine atom by assuming positive linear correlation. Vertical lines for CH_2ClI and CH_2BrI demonstrate the virtual kinetic values ($-\log k_{virtual}$) for clarity.

decomposition rate of lithium halocarbenoids **2**, and then investigated the correlation between the calculated parameters closely related to the decomposition.

We employed the rate for the homolytic cleavage of carbenoid **2** giving two separate radicals **5** and **6**, obtained simply by *ab initio* calculation, as the simplest parameter for evaluating the correlation (eqn (4)). Structural optimization of the molecules was performed at the MP2/6-311G(d,p) level,[12] which was further subjected to single-point calculation to evaluate the zero-point corrected energy (ΔE_0) at the CCSD(T)/aug-cc-pVDZ level (aug-cc-pVDZ-PP for the I atom).[13] The calculated energies (ΔE_0, eqn (5)) were then conveniently converted into virtual reaction rates ($k_{virtual}$) using the Eyring–Polanyi equation (eqn (6)) to evaluate the correlation with the real kinetic rates (k_{exp}) determined using the flash quench-flow method (eqn (7)). Although the virtual rates do not reflect the experimental rates because they are not based on realistic models, surprisingly, a double logarithmic plot of both reaction rates for the three types of dihalomethanes bearing two identical halogen atoms showed a strong linear correlation when fitted using the least-squares approximation (R^2 = 0.998; Fig. 2). These observations suggest that the kinetic stabilities of C1 carbenoids composed of various halogen atoms can be explained by statistical predictions based on simple calculations that do not involve realistic molecular models.

$$\underset{\mathbf{2}}{\mathrm{LiCHX^1{-}X^2}} \rightarrow \underset{\mathbf{5}}{\mathrm{LiCHX^1\cdot}} + \underset{\mathbf{6}}{\mathrm{\cdot X^2}} \quad (4)$$

$$\Delta E_0 = E_{ZPE}(\mathbf{5}) + E_{ZPE}(\mathbf{6}) - E_{ZPE}(\mathbf{2}) \quad (5)$$

$$k_{virtual} = \frac{k_B T}{h} \exp\left(\frac{-\Delta E_0}{RT}\right) \quad (6)$$

$$\log k_{exp} \propto \log k_{virtual} \quad (7)$$

We hypothesise that the linear correlation tendency in eqn (7) can be extended to a similar series of halocarbenoids.

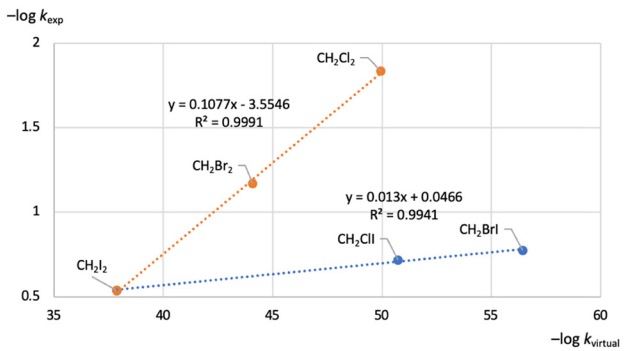

Fig. 3 Linear regression for experimental (−log k_{exp}) and theoretical (−log $k_{virtual}$) kinetic rates for decomposition of lithium halocarbenoids **2a–e** at −20 °C.

Table 1 Bond dissociation energies and decomposition rates for the dihalomethyllithium species at −20 °C

Carbenoid	Calcd ΔE_0 (kcal mol^{-1})	$k_{virtual}$ (s^{-1})	k_{exp} (s^{-1})
LiCHI–I	58.6	5.1×10^{-43}	2.9×10^{-1}
LiCHBr–Br	65.8	9.3×10^{-50}	6.7×10^{-2}
LiCHCl–Cl	72.6	4.2×10^{-56}	1.5×10^{-2}
LiCHBr–I	80.3	2.7×10^{-63}	1.7×10^{-1}
LiCHCl–I	73.5	6.7×10^{-57}	1.9×10^{-1}

Subsequent investigations began by predicting the order of stability of the halocarbenoids (**2d** and **2e**) derived from the deprotonation of iodine-containing dihalomethanes (X^2 = I) by calculating the energy of homolytic cleavage. The predicted decomposition rates from the calculated C–I bond dissociation energy are in the counterintuitive order of CH_2I–I (E_0 = 58.6 kcal mol^{-1}) > CH_2Cl–I (73.5 kcal mol^{-1}) > CH_2Br–I (80.3 kcal mol^{-1}). Notably, this order does not follow the intuitive stability of the C–X^1 bond, because the decomposition of lithium halocarbenoids may be directly related to the cleavage of the C–I (X^2) bond. The actual decomposition rates measured with quench-flow kinetics have a strong positive correlation with those obtained by calculation (R^2 = 0.994), which means that the binding energy of the C–I bonds is also correlated with the actual kinetic decomposition rates of iodine-containing halocarbenoids (Fig. 3 and Table 1).

Based on this trend, we attempted to predict the reaction rates at various temperatures solely based on the correlation gradients and the kinetic data that we reported previously for the diiodomethyl lithium intermediate (1.5×10^0 s^{-1} at 0 °C and 8.1×10^{-2} s^{-1} at −40 °C).[11h] Predicting the reactivity of active species in molecular systems with different constituent elements is challenging. However, the reaction rates predicted for other temperature ranges showed remarkably accurate correlations with the actual measured rates (Table 2 and Fig. 4). This type of predictive approach can be highly valuable for comprehensively and integratively understanding

Table 2 Prediction of decomposition rates for the dihalomethyllithium species at different temperatures

Carbenoid	T (°C)	$k_{predict}$ (s^{-1})	k_{exp} (s^{-1})
LiCHI–I	−20	—	2.9×10^{-1}
LiCHBr–Br	−20	—	6.7×10^{-2}
LiCHCl–Cl	−20	—	1.5×10^{-2}
LiCHBr–I	−20	—	1.7×10^{-1}
LiCHCl–I	−20	—	1.9×10^{-1}
LiCHI–I	0	—	1.5×10^{0}
LiCHBr–Br	0	3.2×10^{-1}	2.8×10^{-1}
LiCHCl–Cl	0	7.5×10^{-2}	7.4×10^{-2}
LiCHBr–I	0	8.6×10^{-1}	6.0×10^{-1}
LiCHCl–I	0	1.0×10^{0}	1.0×10^{0}
LiCHI–I	−40	—	8.1×10^{-2}
LiCHBr–Br	−40	1.7×10^{-2}	1.1×10^{-2}
LiCHCl–Cl	−40	4.0×10^{-3}	2.1×10^{-3}
LiCHBr–I	−40	4.6×10^{-2}	2.1×10^{-2}
LiCHCl–I	−40	5.5×10^{-2}	4.3×10^{-2}

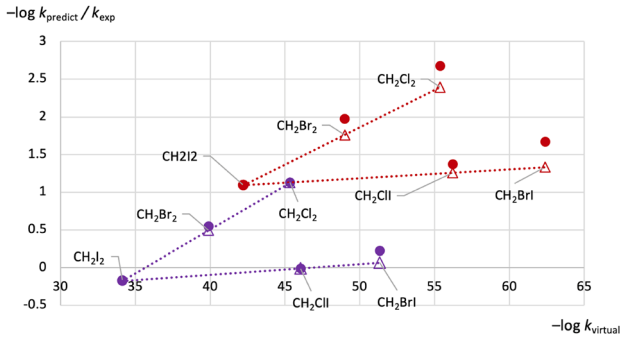

Fig. 4 Prediction plot at different temperatures and comparison to the experimentally determined values. Circle dot: Experimental kinetic values compared to the corresponding virtual kinetic values. Outlined triangle dot: Predicted values compared to the corresponding virtual kinetic values. Red color: −40 °C, purple color: 0 °C.

the reactivity of closely related active species, potentially contributing significantly to the advancement of active species chemistry.

Furthermore, the fact that the same linear trend was observed across different temperature ranges indicates that the decomposition reaction in the present study correctly obeyed first-order decay and fully conformed to the Eyring–Polanyi reaction rate theory. This interpretation is supported by the reaction rates obtained from our flash flow reaction system and represents true kinetic reactivity, which is minimally influenced by physical factors such as mixing and thermal/mass diffusion. This outcome suggests a potentially new theoretical model that can provide a rational explanation for the real reactivity of short-lived and highly reactive species that exist only for extremely short timeframes. Such a model would significantly enhance our understanding of the disguised nature of active fleet species.

Finally, we illustrate the fully analysed temperature-residence time mapping for all dihalomethanes (Fig. 5). We also performed an Arrhenius plot analysis of the reaction rates observed across various temperature ranges. The obtained activation energies E_a exhibited a strong linear correlation with the bond dissociation energy E_0, similar to the plots of the reaction rates (Fig. 6).[14] These findings may imply the involvement of homolytic characteristics in the decomposition process of the active species, in which the reaction rates have good correlation to those predicted in the simplified models for the homolytic cleavage of C–X bonds. This insight may also challenge the traditional interpretation of the decomposition behaviours of lithium carbenoid

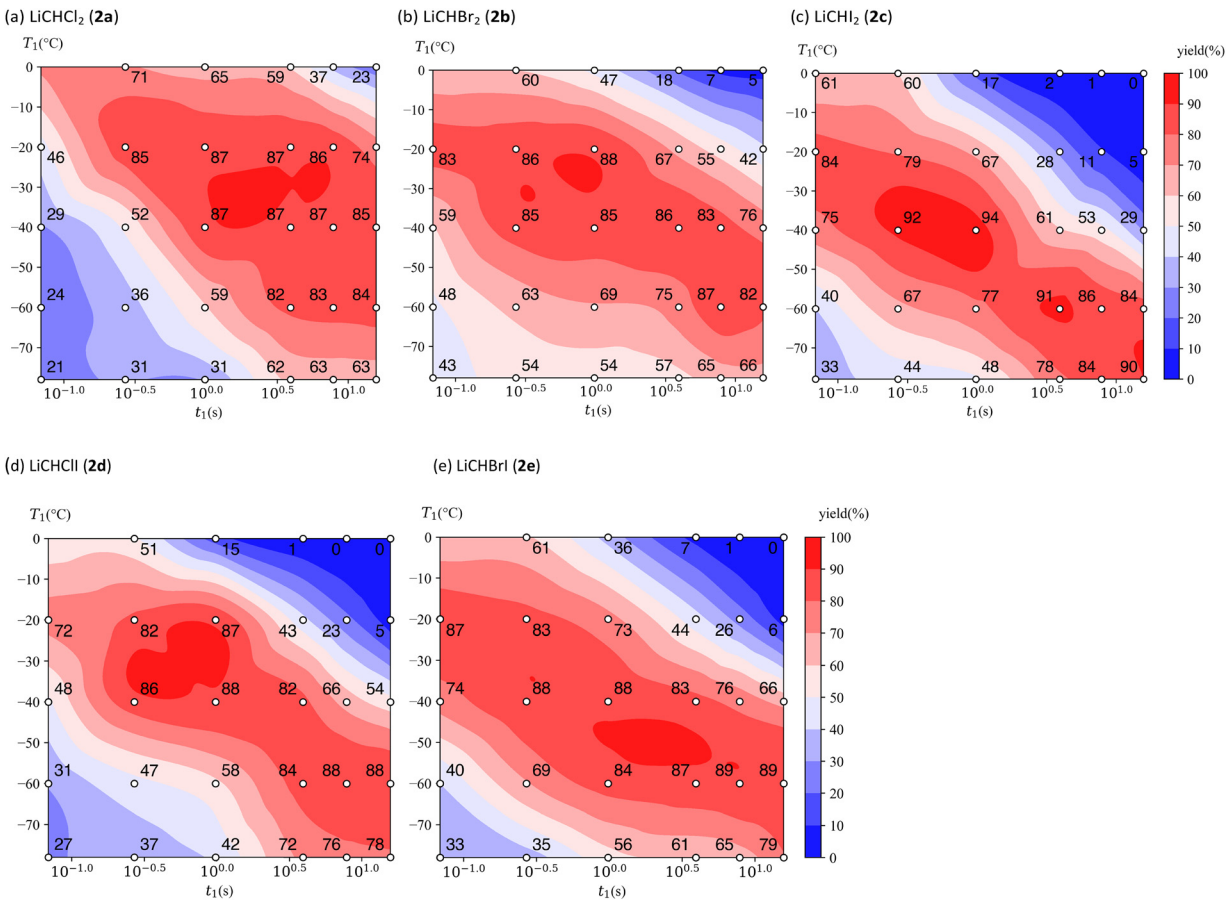

Fig. 5 Temperature-residence time contour mapping for the deuterium-quenching reaction of dihalomethyllithium intermediates **2a**–**e**. The designated number on the outlined circle dot: the yield for monodeuteration product (%).

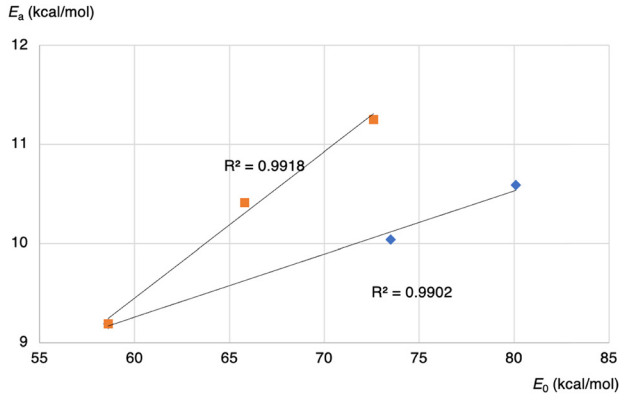

Fig. 6 Activation energy calculated using Arrhenius plot.

species as predominantly heterolytic, thereby casting new light on their reactivity.

In summary, we developed calculation models for the systematization of short-lived carbenoid reactivity by combining theoretical and experimental approaches with statistical correlation. The present methodology for evaluating reaction rates from simple calculation models, such as bonding energies, will provide reasonable and reliable interpretations of unknown reactive species owing to their ultrashort lifetimes. Further *in silico* and *in vitro* studies, using more precise data on the reactivity of C1 carbenoids, are currently ongoing.

Conflicts of interest

There are no conflicts to declare.

Acknowledgements

This work was supported by JSPS KAKENHI Grant Numbers, JP23K04744 (Grant-in-Aid for Scientific Research (C)), JP20KK0121 (Fostering Joint International Research (B)), JP21H01936 (Grant-in-Aid for Scientific Research (B)), JP21H01706 (Grant-in-Aid for Scientific Research (B)), and JP21H05080 (Grant-in-Aid for Transformative Research Areas (B)). This work was also partially supported by AMED (JP21ak0101156), the Core Research for Evolutional Science and Technology (CREST, JPMJCR18R1), New Energy and Industrial Technology Development Organization (NEDO, PJ22031410 and PJ22220030), the Japan Keirin Autorace Foundation, the Ogasawara Foundation for the Promotion of Science & Engineering, and Takahashi Industrial and Economic Foundation.

Notes and references

1 (*a*) H. Siegel, Lithium halocarbenoids—carbanions of high synthetic versatility, *Top. Curr. Chem.*, 2005, **106**, 55–78; (*b*) Modern Lithium Carbenoid Chemistry, in *Contemporary Carbene Chemistry*, ed. R. A. Moss and M. P. Doyle, John Wiley & Sons, 2014, ch. 11; (*c*) V. Capriati and S. Florio, *Chem. – Eur. J.*, 2010, **16**, 4152–4162; (*d*) V. H. Gessner, *Chem. Commun.*, 2016, **52**, 12011–12023; (*e*) V. Pace, W. Holzer and N. De Kimpe, *Chem. Rec.*, 2016, **16**, 2061–2076; (*f*) M. Colella, A. Nagaki and R. Luisi, *Chem. – Eur. J.*, 2020, **26**, 19–32.

2 (*a*) S. P. Thomas, R. M. French, V. Jheengut and V. K. Aggarwal, *Chem. Rec.*, 2009, **9**, 24–39; (*b*) H. K. Scott and V. K. Aggarwal, *Chem. – Eur. J.*, 2011, **17**, 13124–13132; (*c*) D. Leonari and V. K. Aggarwal, *Acc. Chem. Res.*, 2014, **47**, 3174–3183; (*d*) B. S. L. Collins, C. M. Wilson, E. L. Myers and V. K. Aggarwal, *Angew. Chem., Int. Ed.*, 2017, **56**, 11700–11733; (*e*) L. Castoldi, S. Monticelli, R. Senatore, L. Lelo and V. Pace, *Chem. Commun.*, 2018, **54**, 6692–6704; (*f*) D. S. Matteson, B. S. L. Collins and V. K. Aggarwal, *Org. React.*, 2021, **105**, 427–860; (*g*) K. Yeung, R. C. Mykura and V. K. Aggarwal, *Nat. Synth.*, 2022, **1**, 117–126.

3 (*a*) F. Jensen, *Introduction to Computational Chemistry*, Wiley, 3rd edn, 2017, ch. 13; (*b*) N. Koga and K. Morokuma, *Chem. Rev.*, 1991, **91**, 823; (*c*) K. N. Houk and P. H.-Y. Cheong, *Nature*, 2008, **455**, 309; (*d*) H. B. Schlegel, *WIREs Comput. Mol. Sci.*, 2011, **1**, 790; (*e*) S. Maeda, Y. Harabuchi, Y. Ono, T. Taketsugu and K. Morokuma, *Int. J. Quantum Chem.*, 2015, **115**, 258–269.

4 (*a*) S. Maeda and K. Morokuma, *J. Chem. Phys.*, 2010, **132**, 241102; (*b*) S. Maeda, K. Ohno and K. Morokuma, *Phys. Chem. Chem. Phys.*, 2013, **15**, 3683–3701; (*c*) S. Maeda and Y. Harabuchi, *WIREs Comput. Mol. Sci.*, 2021, **11**, e1538; (*d*) H. Hayashi, S. Maeda and T. Mita, *Chem. Sci.*, 2023, **14**, 11601–11616.

5 For examples of quantum calculation studies on lithium carbenoid species, see: (*a*) D. L. Phillips and W.-H. Fang, *J. Org. Chem.*, 2001, **66**, 5890–5896; (*b*) L. M. Pratt, S. Merry, S. C. Nguyen, P. Quanb and B. T. Thanh, *Tetrahedron*, 2006, **62**, 10821–10828; (*c*) Z. Ke, C. Zhao and D. L. Phillips, *J. Org. Chem.*, 2007, **72**, 848–860; (*d*) S. Essafi, S. Tomasi, V. K. Aggarwal and J. N. Harvey, *J. Org. Chem.*, 2014, **79**, 12148–12158; (*e*) Y. Shao, X. Huang, C. Zhao and Z. Ke, *J. Organomet. Chem.*, 2018, **864**, 110–114; (*f*) D. Villablanca, R. Durán, A. M. Lamsabhi and B. Herrera, *ACS Omega*, 2019, **4**, 19452–19461.

6 For reviews on the organolithium aggregation, see: (*a*) *The chemistry oforganolithium compounds*, ed. Z. Rappoport and I. Marek, John Wiley & Sons Ltd, West Sussex, England, 2004; (*b*) V. H. Gessner, C. Däschlein and C. Strohmann, *Chem. – Eur. J.*, 2009, **15**, 3320–3334; (*c*) K. Götz, V. H. Gessner, C. Unkelbach, M. Kaupp and C. Strohmann, *Z. Anorg. Allg. Chem.*, 2013, **639**, 2077–2085.

7 For examples of integrative studies on microflow experiments with statistical data analyses, see: (*a*) C. W. Coley, D. A. Thomas III, J. A. M. Lummiss, J. N. Jaworski, C. P. Breen, V. Schultz, T. Hart, J. S. Fishman, L. Rogers, H. Gao, R. W. Hicklin, P. P. Plehiers, J. Byington, J. S. Piotti, W. H. Green, A. J. Hart, T. F. Jamison and K. F. Jensen, *Science*, 2019, **365**, 557; (*b*) M. Kondo, H. D. P. Wathsala, M. Sako, Y. Hanatani, K. Ishikawa, S. Hara, T. Takaai, T. Washio, S. Takizawa and H. Sasai, *Chem. Commun.*, 2020, **56**, 1259; (*c*) N. Sugisawa, H. Sugisawa, Y. Otake, R. V. Krems, H. Nakamura and S. Fuse, *Chemistry–Methods*, 2021, **1**, 484–490;

(*d*) E. Sato, M. Fujii, H. Tanaka, K. Mitsudo, M. Kondo, S. Takizawa, H. Sasai, T. Washio, K. Ishikawa and S. Suga, *J. Org. Chem.*, 2021, **86**, 16035–16044; (*e*) P. Sagmeister, R. Lebl, I. Castillo, J. Rehrl, J. Kruisz, M. Sipek, M. Horn, S. Sacher, D. Cantillo, J. D. Williams and C. O. Kappe, *Angew. Chem., Int. Ed.*, 2021, **60**, 8139; (*f*) Y. Naito, M. Kondo, Y. Nakamura, N. Shida, K. Ishikawa, T. Washio, S. Takizawa and M. Atobe, *Chem. Commun.*, 2022, **58**, 3893; (*g*) Y. Ashikari, T. Tamaki, Y. Takahashi, Y. Yao, M. Atobe and A. Nagaki, *Front. Chem. Eng.*, 2022, **3**, 819752.

8 For recent reviews on flow microreactor synthesis, see: (*a*) *Organometallic Flow Chemistry: In Topics in Organometallic Chemistry*, ed. T. Nöel, Springer, Switzerland, 2016; (*b*) M. B. Plutschack, B. Pieber, K. Gilmore and P. H. Seeberger, *Chem. Rev.*, 2017, **117**, 11796; (*c*) D. Cantillo and C. O. Kappe, *React. Chem. Eng.*, 2017, **2**, 7; (*d*) T. Zhao, L. Micouin and R. Piccardi, *Helv. Chim. Acta*, 2019, **102**, e1900172; (*e*) N. Sugisawa, H. Nakamura and S. Fuse, *Catalysts*, 2020, **10**, 1321; (*f*) M. Power, E. Alcock and G. P. McGlacken, *Org. Process Res. Dev.*, 2020, **24**, 1814–1838; (*g*) J. Jiao, W. Nie, T. Yu, F. Yang, Q. Zhang, F. Aihemaiti, T. Yang, X. Liu, J. Wang and P. Li, *Chem. – Eur. J.*, 2021, **27**, 4817–4838; (*h*) A. Nagaki, Y. Ashikari, M. Takumi and T. Tamaki, *Chem. Lett.*, 2021, **50**, 485–492; (*i*) Y. Ashikari and A. Nagaki, *Synthesis*, 2021, **53**, 1879–1888; (*j*) W. C. Fu, P. M. MacQueenac and T. F. Jamison, *Chem. Soc. Rev.*, 2021, **50**, 7378–7394; (*l*) Y. Ashikari and A. Nagaki, in *Enabling Tools and Techniques for Organic Synthesis: A Practical Guide to Experimentation, Automation, and Computation*, ed. S. G. Newman, John Wiley & Sons, Hobouken, 2023, ch. 4, pp. 107–147.

9 For selected examples of microflow synthesis, see: (*a*) G. Laudadio, Y. Deng, K. van der Wal, D. Ravelli, M. Nuño, M. Fagnoni, D. Guthrie, Y. Sun and T. Noël, *Science*, 2020, **369**, 92–96; (*b*) S. Chatterjee, M. Guidi, P. H. Seeberger and K. Gilmore, *Nature*, 2020, **579**, 379–384; (*c*) H. Miyamura and S. Kobayashi, *Angew. Chem.*, 2022, **61**, e202201203; (*d*) Y. Jiang and H. Yorimitsu, *JACS Au*, 2022, **2**, 2514–2521; (*e*) O. Shamoto, K. Komuro, N. Sugisawa, T.-H. Chen, H. Nakamura and S. Fuse, *Angew. Chem.*, 2023, **62**, e202300647; (*f*) Y. Jiang, T. Kurogi and H. Yorimitsu, *Nat. Synth.*, 2023, DOI: **10.1038/s44160-023-00439-8**.

10 For recent examples of the flash flow organolithium chemistry, see: (*a*) H. Kim, A. Nagaki and J. Yoshida, *Nat. Commun.*, 2011, **2**, 264; (*b*) Y. Tomida, A. Nagaki and J. Yoshida, *J. Am. Chem. Soc.*, 2011, **133**, 3744; (*c*) J. Wu, X. Yang, Z. He, X. Mao, T. A. Hatton and T. F. Jamison, *Angew. Chem., Int. Ed.*, 2014, **53**, 8416–8420; (*d*) A. Nagaki, Y. Takahashi and J. Yoshida, *Angew. Chem., Int. Ed.*, 2016, **55**, 5327; (*e*) A. Nagaki, H. Yamashita, K. Hirose, Y. Tsuchihashi and J. Yoshida, *Angew. Chem., Int. Ed.*, 2019, **58**, 4027; (*f*) D. Ichinari, Y. Ashikari, K. Mandai, Y. Aizawa, J. Yoshida and A. Nagaki, *Angew. Chem., Int. Ed.*, 2020, **59**, 1567; (*g*) M. Colella, A. Tota, Y. Takahashi, R. Higuma, S. Ishikawa, L. Degennaro, R. Luisi and R. A. Nagaki, *Angew. Chem., Int. Ed.*, 2020, **59**, 10924; (*h*) Y. Ashikari, T. Kawaguchi, K. Mandai, Y. Aizawa and A. Nagaki, *J. Am. Chem. Soc.*, 2020, **142**, 17039; (*i*) Y. Ashikari, T. Tamaki, T. Kawaguchi, M. Furusawa, Y. Yonekura, S. Ishikawa, Y. Takahashi, Y. Aizawa and A. Nagaki, *Chem. – Eur. J.*, 2021, **27**, 16107–16111; (*j*) A. Kremsmair, H. R. Wilke, J. H. Harenberg, B. R. G. Bissinger, M. M. Simon, N. Alandini and P. Knochel, *Angew. Chem., Int. Ed.*, 2023, **62**, e202214377; (*k*) K. Muta, K. Okamoto and A. Nagaki, *Synlett*, 2023, DOI: **10.1055/a-2170-2976**.

11 For recent examples of the carbenoid species using flow chemistry, see: (*a*) J. Hartwig, J. B. Metternich, N. Nikbin, A. Kirschning and S. V. Ley, *Org. Biomol. Chem.*, 2014, **12**, 3611–3615; (*b*) A. Hafner, V. Mancino, M. Meisenbach, B. Schenkel and J. Sedelmeier, *Org. Lett.*, 2017, **19**, 786–789; (*c*) G. Parisi, M. Colella, S. Monticelli, G. Romanazzi, W. Holzer, T. Langer, L. Degennaro, V. Pace and R. Luisi, *J. Am. Chem. Soc.*, 2017, **139**, 13648–13651; (*d*) T. von Keutz, D. Cantillo and C. O. Kappe, *Org. Lett.*, 2019, **21**, 10094–10098; (*e*) P. Musci, M. Colella, A. Sivo, G. Romanazzi, R. Luisi and L. Degennaro, *Org. Lett.*, 2020, **22**, 3623–3627; (*f*) T. von Keutz, D. Cantillo and C. O. Kappe, *Org. Lett.*, 2020, **22**, 7537–7541; (*g*) M. Colella, A. Tota, Y. Takahashi, R. Higuma, S. Ishikawa, L. Degennaro, R. Luisi and A. Nagaki, *Angew. Chem.*, 2020, **59**, 10924–10928; (*h*) K. Okamoto, R. Higuma, K. Muta, K. Fukumoto, Y. Tsuchihashi, Y. Ashikari and A. Nagaki, *Chem. – Eur. J.*, 2023, **29**, e202301738.

12 Y. G. Lazarou, A. V. Prosmitis, V. C. Papadimitriou and P. Papagiannakopoulos, *J. Phys. Chem. A*, 2001, **105**, 6729.

13 K. A. Peterson, B. C. Shepler, D. Figgen and H. Stoll, *J. Phys. Chem. A*, 2006, **110**, 13877.

14 For examples of the integrative studies using calculative bonding energies for linear correlation to experimental values, see: (*a*) M. E. Evans, C. L. Burke, S. Yaibuathes, E. Clot, O. Eisenstein and W. D. Jones, *J. Am. Chem. Soc.*, 2009, **131**, 13464–13473; (*b*) E. Clot, C. Mégret, O. Eisenstein and R. N. Perutz, *J. Am. Chem. Soc.*, 2009, **131**, 7817–7827; (*c*) Q. Lu, H. Yuz and Y. Fu, *Chem. Commun.*, 2013, **49**, 10847–10849.